(9) M. Rocha e Silva, *Chemotherapia*, **3**, 544(1961).
(10) J. C. Castillo and E. J. DeBeer, *J. Pharmacol. Exptl. Therap.*, **90**, 104(1947).
(11) R. F. Carlyle, *Brit. J. Pharmacol.*, **21**, 137(1963).
(12) C. A. Stone, H. C. Wenger, C. T. Ludden, J. M. Stavorski, and C. A. Ross, *J. Pharmacol. Exptl. Therap.*, **131**, 73(1961).

ACKNOWLEDGMENTS AND ADDRESSES

Received April 24, 1969, from the *Division of Pharmacology, Pharmacy Research Institute, The University of Connecticut, Storrs, CT 06268*

Accepted for publication June 27, 1969.

Presented to the Pharmacology and Biochemistry Section, APhA Academy of Pharmaceutical Sciences, Montreal meeting, May 1969.

This work was supported by grant AM 11861-02 from the National Institute of Arthritis and Metabolic Diseases, United States Public Health Service.

* Present address: Department of Physiology and Pharmacology, School of Pharmacy, University of the Pacific, Stockton, CA 95204

Interpretation of Percent Dissolved–Time Plots Derived from *In Vitro* Testing of Conventional Tablets and Capsules

JOHN G. WAGNER

Abstract □ It is shown that under sink conditions a percent dissolved value at time t may simply be equivalent to the percent surface area generated to time t. If this is so, then percent dissolved-time data may best be described by a distribution function and the parameters of the distribution employed to describe the data. Simulated percent dissolved-time data, generated by means of the logarithmic normal distribution function, are shown to yield apparent first-order plots. Hence, if the new concept is correct, apparent first-order kinetics, derived from *in vitro* dissolution tests on conventional tablets and capsules, may be an artifact in some cases. In the special case when surface area of drug available for dissolution decreases exponentially with time after some lag time, t_0, then first-order kinetics appear applicable to the dissolution data. Relationships between many of the constants in formerly derived dissolution rate equations and some equations derived in this report are shown. Dimensions of the constants are clarified. The new method of dissolution rate data examination is capable of providing characterizing parameters of greater potential utility than conventional treatments heretofore used.

Keyphrases □ Tablets, capsules—percent dissolved-time plots interpreted □ First-order dissolution rate equation—sink conditions □ Surface area effects—dissolution rates □ Lag time—dissolution rates □ Distribution parameter, relation—dissolution data

Although there is extensive literature on dissolution rate theory it is appropriate here to review some of the equations in order to show relationships between some of the constants and establish their dimensions.

Quantitative Studies

Conditions of Constant Surface Area—Noyes and Whitney (1) quantitatively studied dissolution by rotating cylinders of benzoic acid and lead chloride in water, then analyzing the solution at intervals of time. In their experiments the surface area of chemical available for dissolution remained essentially constant. They showed that dissolution obeyed the equation

$$dC/dt = k\,(C_s - C) \qquad \text{(Eq. 1)}$$

where C is the concentration of solute at time t, C_s is the equilibrium solubility of the solute at the experimental temperature, and k is a first-order rate constant with dimension 1/time. In later experiments (2, 3) the surface area of solute available for dissolution, S, was incorporated into the equation to give

$$dC/dt = k_1 S\,(C_s - C) \qquad \text{(Eq. 2)}$$

where k_1 is a constant with dimensions length²/time. It should be noted that $k = k_1 S$ whence $k_1 = k/S$. Brunner (4) used Fick's law of diffusion to establish a relationship between the constants k and k_1 in the above equations and other variables. These relationships were:

$$k = DS/Vh \qquad \text{(Eq. 3)}$$

$$k_1 = D/Vh \qquad \text{(Eq. 4)}$$

where D is the diffusion coefficient of the solute in the dissolution medium, V is the volume of the dissolution medium, and h is the thickness of the diffusion layer. Equation 1 of Noyes and Whitney was written by Hixson and Crowell (5) as

$$dW/dt = KS\,(C_s - C) \qquad \text{(Eq. 5)}$$

where W is the amount of solute in solution at time t, dW/dt is the rate of appearance of solute in the solution at time t, and K is a constant with dimensions length/time. Equation 5 is obtained from from Eq. 2 by multiplying both sides by V and letting $K = k_1 V$. By comparing terms we find:

$$K = D/h \qquad \text{(Eq. 6)}$$

Equation 5 may be written as

$$dW/dt = KS/V\,(VC_s - W) = k\,(VC_s - W) \qquad \text{(Eq. 7)}$$

If a constant surface dosage form is studied under nonsink and nonreactive conditions then Eq. 7 should apply and the equation may be integrated to give

$$W = VC_s\,(1 - e^{-kt}) \qquad \text{(Eq. 8)}$$

Rearrangement of Eq. 8 and the taking of logarithms of both sides of the rearranged equation leads to:

$$\log\,(VC_s - W) = \log VC_s - \frac{k}{2.303}\,t \qquad \text{(Eq. 9)}$$

It should be noted that under conditions of constant surface area, nonsink, and nonreactive conditions, the asymptote is VC_s and not W^0 (the initial amount of drug in the dosage form) or W^∞ (the amount of drug ultimately dissolved at time infinity).

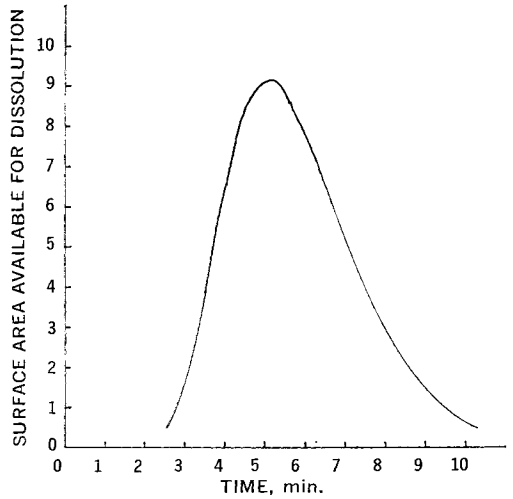

Figure 1—*A simulated plot of surface area available for dissolution* versus *time generated with the logarithmic normal distribution function. See Example No. 1 in* Experimental *section for details.*

Under sink conditions (*i.e.*, $C \ll C_s$, usually $C \leq 0.10C_s$) Eq. 5 simplifies to:

$$dW/dt = KSC_s \qquad \text{(Eq. 10)}$$

Equation 10 indicates that if surface area is held constant under sink and nonreactive conditions then rate of dissolution is constant (*i.e.*, kinetics are zero-order). Equation 10 may be integrated to give:

$$W = KSC_s\, t \qquad \text{(Eq. 11)}$$

Equation 11 indicates that under these conditions a plot of W *versus* t will yield a straight line with slope equal to KSC_s.

After a study of drug release from nonconventional tableted wax matrices under sink conditions Schwartz *et al.* (6) showed that linear plots were obtained when the amount of drug released per unit surface area of the disk exposed to the solvent was plotted against the square root of time. This type of plot was based on the T. Higuchi equation (7) for release of drug from an insoluble, inert matrix. In the previous symbolism of this report this equation is:

$$\frac{W}{S} = \sqrt{\frac{D\epsilon}{\tau}(2A - \epsilon C_s)\, C_s t} \qquad \text{(Eq. 12)}$$

where ϵ is the porosity and τ is the tortuosity of the matrix, A is the concentration of solid drug in the matrix, and the other symbols have the same meanings as defined above. These authors also showed that when log $(W^\infty - W)$ was plotted *versus* t the terminal points

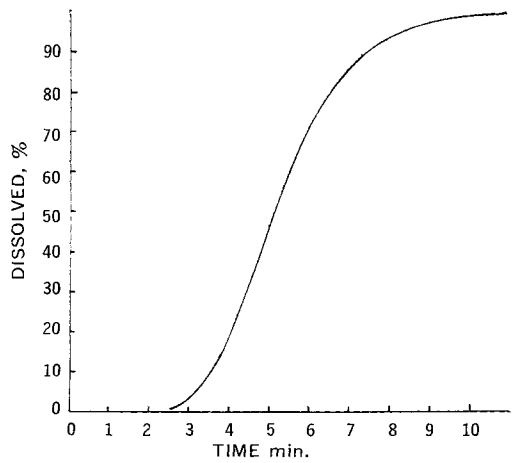

Figure 2—*A simulated percent dissolved* versus *time plot based on the data shown in Fig. 1 and Eq. 20.*

appeared to fall on a straight line but the initial points (early time values) formed a curve above the line.

Conditions of Variable Surface Area—Hixson and Crowell (5) showed that if there is no change in shape of solid during dissolution, the surface area can be related to weight of undissolved drug by means of shape-volume factors and they derived their well-known "cube root law." The contributions of these amd many other investigators to dissolution rate theory have been reviewed by several authors (8–11).

In 1959, Wagner (12) showed that most sustained-action dosage forms, for which release-time data had been reported in the literature hithertofore, released their contained drug to fluids in the *in vitro* tests at pseudo- (or apparent-) first-order rates. This concept was extended to conventional tablets by Schroeter *et al.* (13). Subsequently, it has become rather common practice to plot data derived from dissolution rate studies on conventional tablets and capsules in conformity with first-order kinetics. Usually the percent drug not dissolved (*i.e.*, 100% − dissolved) is plotted on the logarithmic scale of semilogarithmic graph paper against time in minutes on the abcissa. Frequently the data points are nonlinear in the early time period, but, at later times, a straight line usually may be fitted to the data points. Such apparent first-order plots are obtained under sink conditions, as has been pointed out by Gibaldi and Feldman (14). However, the dissolution of a quantity of drug, from a dosage form which releases drug in a quantity of solvent which is just sufficient to dissolve the total amount of drug in the dosage form, may obey apparent second-order kinetics (14, 15).

THEORETICAL

New Approach to Derivation of the First-Order Rate Equation—For the case when there are sink conditions and surface area varies with time one may assume that during the first-order phase of dissolution the surface area available for dissolution decreases exponentially with time. That is, one may assume:

$$S = S^0 e^{-k_s(t-t_0)} \qquad \text{(Eq. 13)}$$

here S^0 is the surface area available for dissolution at the time when the apparent first-order dissolution phase commences at the time t_0. Substitution for S in Eq. 10 from Eq. 13 yields

$$dW/dt = KC_sS^0e^{-k_s(t-t_0)} \text{ for } t \geq t_0 \qquad \text{(Eq. 14)}$$

Integration of Eq. 14 gives

$$W = W_{t_0} + \frac{K}{k_s} C_sS^0\,[1 - e^{-k_s(t-t_0)}] = W_{t_0} + M[1 - e^{-k_s(t-t_0)}] \text{ for } t \geq t_0 \qquad \text{(Eq. 15)}$$

where W_{t_0} is the amount dissolved at time t_0 and $M = (K/k_s)C_sS^0$ and has dimension of mass. Thus, $W^\infty = W_{t_0} + M$ where W^∞ is the amount in solution at infinite time: rearrangement of Eq. 15 and substitution of W^∞ for $W_{t_0} + M$ yields:

$$W^\infty - W = Me^{-k_s(t-t_0)} \text{ for } t \geq t_0 \qquad \text{(Eq. 16)}$$

Taking logarithms of both sides of Eq. 16 gives Eq. 17.

$$\log (W^\infty - W) = \log M - \frac{k_s}{2.303}(t - t_0) \text{ for } t \geq t_0 \qquad \text{(Eq. 17)}$$

where $W^\infty - W$ is the amount not dissolved from the dosage form. Equation 17 provides a basis for the apparent first-order plots mentioned above. A similar equation to Eq. 17 was derived by Gibaldi and Feldman (14). In their derivation they assumed that the surface area was proportional to the weight of undissolved drug, *i.e.*, $S \propto (W^\infty - W)$. A similar assumption was made by Raghunathan and Becker (15) in their derivation of a second-order rate equation.

New Approach to Interpretation of Percent Dissolved-Time Plots—It is feasible that the apparent first-order plots obtained from *in vitro* testing of conventional tablets and capsules are artifacts. The scheme usually written for the processes involved in such *in vitro* tests is as follows:

drug in dosage form $\xrightarrow{\text{disintegration}}$ drug in small particles $\xrightarrow{\text{dissolution}}$ drug in solution

Sheme I

Such sequential schemes imply that dissolution does not occur until the drug is in fine particle form. A modification of the scheme of Aguiar *et al.* (16) seems more appropriate and is shown as Scheme II.

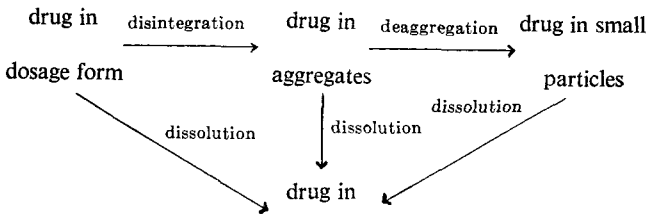

Scheme II

For example, consider a conventional tablet being added to the dissolution medium. Scheme II indicates that dissolution of drug occurs not only from the small particles but also from the intact tablet and the aggregates or granules produced after disintegration. For such a scheme one would expect the surface area of drug available for dissolution to be essentially zero at zero time (since the intact dosage form presents essentially no surface area compared with the surface area eventually generated), then the surface area would increase with increase in time, eventually reach a maximum, then fall off progressively with time until $S \approx 0$ at $t = \infty$.

Under sink and nonreactive conditions one would expect Eq. 10 to hold for each instant of time during the entire process. One may then integrate Eq. 10 between limits $t = 0$ and $t = T$ to yield:

$$W = KC_s \int_0^T S(t)dt \qquad \text{(Eq. 18)}$$

where W is the amount of drug dissolved to some particular time T and the integral represents the cumulative surface area which has been made available for dissolution from time zero to the particular time T. By analogy, at infinite time we obtain:

$$W^\infty = KC_s \int_0^\infty S(t)dt \qquad \text{(Eq. 19)}$$

Hence,

$$\left\{\begin{matrix}\%\text{ dissolved} \\ \text{to time } T\end{matrix}\right\} = \frac{W}{W^\infty} \times 100 = \frac{\int_0^T S(t)dt}{\int_0^\infty S(t)dt} \times 100 = \left\{\begin{matrix}\%\text{ surface area generated to time } T \text{ of} \\ \text{total surface generated}\end{matrix}\right\} \qquad \text{(Eq. 20)}$$

Thus, one may interpret each ordinate value of a percent dissolved-time plot as equivalent to the ratio of the cumulative surface area which has been made available for dissolution up to that time to the total surface area which is made available during the entire test multiplied by 100. In the special case when:

$$\int_{t_0}^T S(t)dt = \int_{t_0}^T S^0 e^{-k_s(t-t_0)}\,dt = \frac{S^0}{k_s}\left[1 - e^{-k_s(T-t_0)}\right] \qquad \text{(Eq. 21)}$$

then first-order kinetics would be observed after the lag time t_0. However, in other cases when Eq. 21 does not hold one would not expect true first-order kinetics. How then may one explain the apparent first-order plots frequently obtained from *in vitro* data? It is feasible that the answer to this question is that such plots are artifacts and arise only because Eq. 13 is an approximation to the $S(t)$, t values past the peak of the $S(t)$, t plot, or, in other words, that Eq. 17, after conversion to percentage values, yields an approximation to the percent dissolved time data. It is extremely important, however, to realize that if this is true, then there is no fundamental first-order process involved as in chemical kinetics. Rather, Eq. 20 indicates the fundamental principle generating the data.

Assuming the validity of Eq. 20 one may then use the percent dissolved-time data directly to determine the distribution of surface

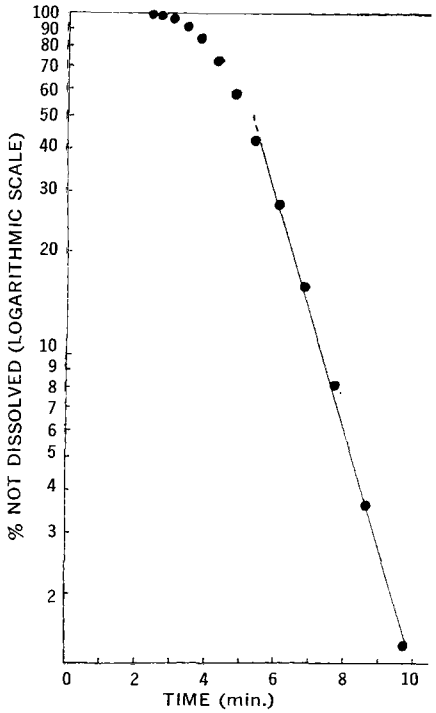

Figure 3—*The data of Fig. 2 plotted in first-order kinetic fashion. See Eq. 26 and text nearby for interpretation.*

area available for dissolution during the *in vitro* test procedure. Scheme II and the text pertaining to it indicates one may expect a distribution of surface area with the following properties: (*a*) the range of surface area would be expected to be closed at the lower end, for example by zero or significant surface area would appear after some lag time required for the capsule shell to break or dissolve or a tablet to start disintegrating; (*b*) the density function (derivative) plot should rise steeply, reach a peak then fall off more slowly than the rise of the up part of the curve, *i.e.*, an asymmetric distribution; and (*c*) effectively open at the upper end but with the cumulative plot reaching an asymptote. The most common types of distributions having these properties are the logarithmic normal distribution and the logarithmic logistic distribution (17–22). However, the distribution of surface area generated by such a process may well be described in some cases by other distribution laws or empirical equations (20), or, of course, the data may not adhere to

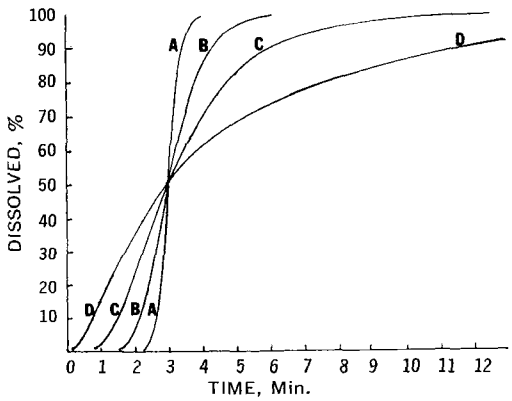

Figure 4—*Four simulated percent dissolved* versus *time plots generated with the logarithmic normal distribution function. For details see Example No. 2 of* Experimental *section. In each case* $\overline{\log_{10}X} = 0.4771$ *(antilog is 3.00, corresponding to* $T_{50\%}$*). Key:*

Code	σ_{10}	$\sigma_{10}/\overline{\log_{10}X}$
A	*0.04771*	*0.10*
B	*0.1193*	*0.25*
C	*0.2386*	*0.50*
D	*0.4771*	*1.00*

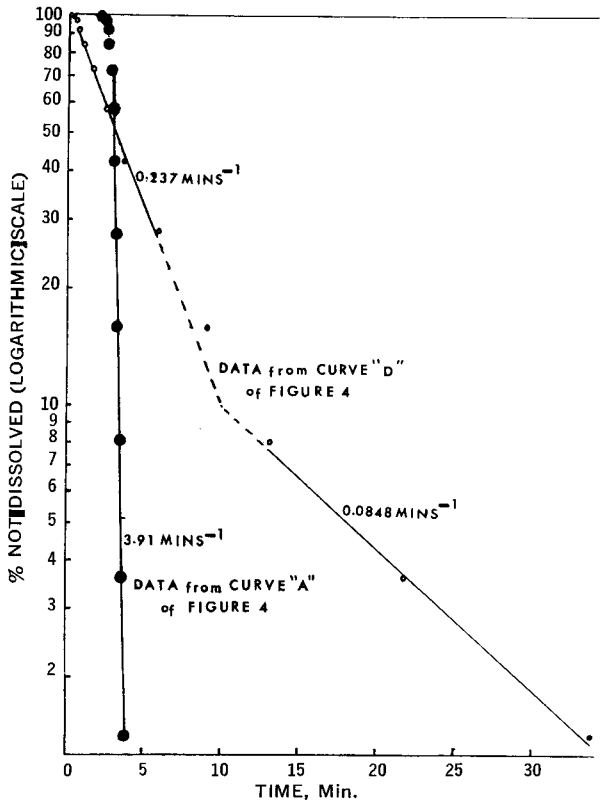

Figure 5—*The data of Curves* A *and* D *of Fig. 4 plotted in first-order kinetic fashion. See Eqs. 27, 28, and 29 and text nearby for interpretation.*

any known distribution function. Both logarithmic normal probability graph paper and logarithmic logistic ruling paper are available commercially (23). To test the theoretical Eq. 20 one would simply plot the cumulative percent dissolved values on the probability scale (ordinate) *versus* the corresponding time values on the logarithmic scale (abscissa). If the data are described by the corresponding distribution function then the points should fall randomly about a straight line which could be drawn through the points. In the case of logarithmic normal graph paper an estimate of the median time may be obtained by reading the time corresponding to the 50% point; an estimate of the *SD* may be obtained from the 16, 50, and 84% points by appropriate conversion of the time values to their logarithms then taking differences. Equations appropriate to the logarithmic normal distribution are given by several authors (17, 18, 20, 24). Equations appropriate to the logarithmic logistic distribution are given by Berkson (22).

EXPERIMENTAL

In order to test whether the logarithmic normal distribution may explain many of the observations made from percent dissolved-time plots generated from *in vitro* testing of conventional tablets and capsules some log-normal distributions were generated and the data plotted in several ways. Data were generated as follows.

Let

$\log X_E$, $\log X_{E1}$, and $\log X_{E2}$ represent abscissa values at the end of intervals;
$\log X_M$ represent abscissa values at the mid points of intervals;
$\overline{\log X}$ represent the average of the logarithms of the X values;
σ_{10} represent the *SD* in log base 10 units;
Z represent the number of *SD*'s measured from the median of the standard normal distribution (usual range is -3 to $+3$);
$N(Z)$, $N(Z_1)$, and $N(Z_2)$ be values of the areas under the standard normal distribution curve from $-\infty$ to Z, Z_1, and Z_2, respectively (see Table I, p. 392 of *Reference* 24 or other statistical textbooks);
Y represent the value plotted on the ordinate scale.

Then,

$$X_E = \text{antilog}\,[\sigma_{10} Z + \overline{\log X}] \qquad \text{(Eq. 22)}$$

$$Y_E = 100\,N(Z) \qquad \text{(Eq. 23)}$$

A set of X_E and Y_E values generated by means of Eqs. 22 and 23 will yield a linear plot when plotted on logarithmic normal probability graph paper and a plot such as shown in Figs. 2 and 4 when plotted on cartesian coordinate graph paper. The plots illustrated in this report were prepared by employing 14 values of Z ranging from -2.6 to $+2.6$ with increments of 0.4.

To prepare density function (derivative) plots, as illustrated in Fig. 1 one uses the data generated by means of Eqs. 22 and 23 as follows:

$$X_M = \text{antilog}\left[\frac{\log X_{E2} - \log X_{E1}}{2}\right] \qquad \text{(Eq. 24)}$$

$$Y_M = \Sigma n\,[N(Z_2) - N(Z_1)] \qquad \text{(Eq. 25)}$$

where Σn is the total number of items and was taken as 58 for Fig. 1 and as 100 in other cases.

Example No. 1—$\overline{\log X}$ was taken as 0.7102, σ_{10} was taken as 0.1263, and Σn was made equal to 58. Eqs. 22–25 yielded the simulated data shown in Fig. 1. The Y_M values from eq. 25 are plotted as surface area available for dissolution on the ordinate and the X_M values from Eq. 24 are plotted as time values on the abscissa.

Applying Eq. 20, the curve shown in Fig. 2 was obtained. Here the Y_E values obtained with Eq. 23 are plotted as percent dissolved on the ordinate and the X_E values obtained with Eq. 22 are plotted as time values on the abscissa. The striking similarity between this simulated curve and many real percent dissolved-time plots is at once apparent.

Figure 3 is a plot of (100% − dissolved) on the logarithmic scale of semilogarithmic graph paper *versus* time in minutes. That is, Fig. 3 is a plot of the same data as shown in Fig. 2. That portion of the data shown in Fig. 1 from the peak onward yielded an apparent straight line in Fig. 3. Least squares linear regression gave the equation:

$$\log (100\%\ \text{dissolved}) = 3.5498 - 0.3467t, \qquad \text{(Eq. 26)}$$

for the terminal sixpoints. The coefficient of determination was 0.997 indicating that 99.7% of the variance of the ordinate values could be accounted for by differences in the abscissa values. The apparent first-order rate constant is 0.798 min.$^{-1}$. However, it is obvious that first-order kinetics are really not involved here at all. Figure 3 is really an artifact.

Example No. 2—Four log-normal distributions were generated—all having the same median. In each case $\overline{\log X}$ was 0.4771 with an antilog of 3 min. corresponding to the median. Values of σ_{10} equal to 0.04771, 0.1193, 0.2386, and 0.4771 were used for the four distributions such that the ratios $\sigma_{10}/\overline{\log X}$ were 0.10, 0.25, 0.50, and 1.00, respectively. The cumulative plots on cartesian coordinate graph paper are shown in Fig. 4. As the *SD* increases from Curve *A* through Curve *D* the curves lean more and more and the apparent lag time decreases—but all four curves pass through the same point corresponding to 50% dissolved at 3 min. The latter value is comparable to the $T_{50\%}$ value of a real percent dissolved-time plot.

Semilogarithmic plots of (100% − dissolved) *versus* time for the data corresponding to Curves *A* and *D* are shown in Fig. 5. Curve *A* of Fig. 4 gave an apparent linear semilogarithmic plot in the range 72.5 to 1.4% not dissolved. Least-squares linear regression gave the equation:

$$\log (100\%\ \text{dissolved}) = 6.7716 - 1.6965t, \qquad \text{(Eq. 27)}$$

from the terminal eight points. The coefficient of determination was 0.972 and the corresponding apparent first-order rate constant was 3.91 min.$^{-1}$. Data from Curve *D* of Fig. 4 appeared to yield two apparently linear segments in Fig. 5. The first segment (early time values) gave the equation:

$$\log (100\% - \text{dissolved}) = 2.0210 - 0.1031t, \qquad \text{(Eq. 28)}$$

with a coefficient of determination of 0.996. The second (later time values) gave the equation:

$$\log (100\% - \text{dissolved}) = 1.3677 - 0.03682t \qquad \text{(Eq. 29)}$$

with a coefficient of determination of 0.998. The apparent first-order rate constants were 0.237 and 0.0848 min.$^{-1}$, respectively.

The fact that real percent dissolved-time data sometimes yields two apparent first-order rates was discussed by Gibaldi (25). However, if the interpretation suggested by Eq. 20 is correct, then the first-order rate constants in such a case are really artifacts. The data shown in Figs. 1, 2 and 4 are best described by the medians and the *SD*'s which are parameters of the log-normal distributions and not by the apparent first-order rate constants obtained by plotting the data as shown in Figs. 3 and 5.

DISCUSSION

Eqs. 18, 19, and 20 may not be exact in application to conventional tablet or capsule dissolution rates for at least two reasons. First, wetting phenomena may in large part be responsible for the initial "foot" observed in many percent dissolved-time plots. Many other factors are also involved initially when the dosage form disintegrates. Hence the equations cited and the laws of probability may not be strictly valid for the very early part of the dissolution curve. Secondly, Higuchi and Hiestand (26) and Goyan (27) have pointed out that the effective diffusion layer thickness, h, may change with particle size, hence K in Eqs. 18 and 19 may not truly be a constant. However, one would expect the greatest change in K, if it occurred, to occur near the end of the dissolution process when the fine particles are very small in size.

By a new method using thermal analysis Nogami *et al.* (28), Nakai and Kubo (29), and Nakai (30) have been able to obtain plots of surface area *versus* time during disintegration and dissolution of compressed tablets. In general their treatment and data support the applicability of Eq. 20 to conventional tablets and capsules. Also, their plots of surface are *versus* time obtained by the thermal analysis method have an asymmetrical shape analogous to Fig. 1 which suggests a possible linearization on logarithmic probability graph paper.

Preliminary trials indicate that real percent dissolved-time data frequently yield linear plots on logarithmic normal graph paper. Examples are as follows. Wood (31) reported on the dissolution rate of aspirin from a commercial tablet (Bufferin) in 0.1 *N* HCl, 0.01 *N*. HCl and pH 7.5 buffer at both a slow stirring speed (30 r.p.m.) and a fast stirring speed (440 r.p.m.). Five of the six sets of data he reported give straight lines on logarithmic probability graph paper when the percent dissolved values are plotted on the probability scale and the time values on the logarithmic scale. The exception was the pH 7.5 buffer–440 r.p.m. data which gave a curved line on logarithmic probability paper but a single straight line when the data were plotted in first-order fashion. The dissolution of griseofulvin from capsules and tablets in simulated intestinal fluid provided data, reported by Katchen and Symchowicz (32), which gave linear plots on logarithmic-probability graph paper. Castello *et al.* (33) reported average percent dissolved-time data for dissolution of twenty individual potassium chloride tablets in pH 7.2 buffer when tested in a new multiple testing station apparatus. These average values gave a linear logarithmic-normal probability plot.

The author is offering the distribution plot concept as another possible way of evaluating percent dissolved-time data derived from the testing of conventional tablets and capsules. If such data is linearized, for example, by plotting on logarithmic-probability graph paper then all the data derived from a given test may be described adequately by the parameters of the distribution such as the median and *SD* in the log-normal case. These parameters may then possibly be used to correlate with *in vivo* data. The importance of this concept with respect to establishment of official rate of dissolution standards and *in vitro-in vivo* correlations is, therefore, evident. For example, the $T_{50\%}$ value above would provide an inadequate description of each set of data shown in Fig. 4. However, if these data were plotted on logarithmic-probability graph paper, the estimated median ($T_{50\%}$) and the *SD* of each distribution would provide adequate descriptions. Another advantage is that, if the data are linearized by logarithmic-probability graph paper, one may readily read off any desired value such as $T_{20\%}$, $T_{50\%}$, $T_{90\%}$, *etc.*

The author does not intend to imply that first-order plots for tablet and capsule dissolution are "out." If data provide single component first-order plots which go through the origin point (100% on logarithmic scale) or very near it then such plots provide an adequate description. Also such data would give a curved line on logarithmic-probability graph paper. However, there are many sets of percent dissolved-time data which yield very poor first-order plots and frequently there appears to be two first-order components; an example is the data of Wood (31) cited above. In these cases the trial of a distribution plot such as the use of logarithmic-normal probability graph paper may be worthwhile. As pointed out, the true distribution will be complex, and generally indeterminate, but often approximated within fixed limits by such distributions as cited. The author wishes to caution against claims of absoluteness of a calculated distribution shape (and differences) based upon fortuitous fits of data to a specific theoretical distribution.

REFERENCES

(1) A. Noyes and W. Whitney, *J. Am. Chem. Soc.*, **19,** 930 (1897).

(2) A. Noyes and W. Whitney, *Z. Physik. Chem.*, **23,** 689 (1897).

(3) L. Bruner and S. Tolloczko, *ibid.*, **35,** 382(1900).

(4) E. Brunner, *ibid.*, **47,** 56(1904).

(5) A. Hixson and J. Crowell, *Ind. Eng. Chem.*, **23,** 923(1931).

(6) J. B. Schwartz, A. P. Simonelli, and W. I. Higuchi, *J. Pharm. Sci.*, **57,** 274(1968).

(7) T. Higuchi, *ibid.*, **52,** 1145 (1963).

(8) J. G. Wagner, *ibid.*, **50,** 359(1961).

(9) D. E. Wurster and P. W. Taylor, *ibid.*, **54,** 169(1965).

(10) W. I. Higuchi, *ibid.*, **56,** 315(1967).

(11) J. H. Fincher, *ibid.*, **57,** 1825(1968).

(12) J. G. Wagner, *Drug Std.*, **27,** 178(1959); *ibid.*, **28,** 30(1960).

(13) L. C. Schroeter, J. E. Tingstad, E. L. Knoechel, and J. G. Wagner, *J. Pharm. Sci.*, **51,** 865(1962).

(14) M. Gibaldi and S. Feldman, *ibid.*, **56,** 1238(1967).

(15) V. Raghunathan and C. H. Becker, *ibid.*, **57,** 1748(1968).

(16) A. J. Aguiar, J. E. Zelmer, and A. W. Kinkel, *ibid.*, **56,** 1243(1967).

(17) J. H. Gaddum, *Nature*, **156,** 473(1945).

(18) J. Moshman, *J. Am. Statistical Assoc.*, **48,** 600(1953).

(19) A. L. Koch, *J. Theoret. Biol.*, **12,** 276(1966).

(20) C. Orr, Jr., "Particulate Technology," Macmillan, New York, N. Y., 1966, pp. 12–18.

(21) D. F. Heath, *Nature*, **213,** 1159(1967).

(22) J. Berkson, *J. Am. Statistical Assoc.*, **48,** 565(1953).

(23) Codex Book Co., Inc., Norwood, Mass. Logarithmic normal paper (catalog No. 31, 376); logarithmic logistic ruling paper (catalog No. 32, 454).

(24) B. W. Lindgren, "Statistical Theory," Macmillan, New York, N. Y., 1962, pp. 89, 392.

(25) M. Gibaldi, "Problems in the *In Vitro* Evaluation of Drugs with Limited Aqueous Solubility," presented at a symposium on "*In Vitro* and *In Vivo* Factors in the Design and Evaluation of Dosage Forms," 5th National meeting of the APhA Academy of Pharmaceutical Sciences, Washington, D. C., November 1968.

(26) W. I. Higuchi and E. N., Hiestand, *J. Pharm. Sci.*, **52,** 67 (1963).

(27) J. E. Goyan, *ibid.*, **54,** 645(1965).

(28) H. Nogami, J. Hasegawa, and Y. Nakai, *Chem. Pharm. Bull.* (Tokyo), **7,** 331, 337(1959).

(29) Y. Nakai and Y. Kubo, *ibid.*, **8,** 634(1960).

(30) Y. Nakai, *ibid.*, **8,** 641(1960).

(31) J. H. Wood, "*In Vitro* Evaluation of the Release from Dosage Forms," presented at the "Eino Nelson Memorial Symposium on Biopharmaceutics," Industrial Pharmacy Section, 113th Annual meeting of the APhA, Dallas, April, 1966.

(32) B. Katchen and S. Symchowicz, *J. Pharm. Sci.*, **56,** 1108 (1967).

(33) R. A. Castello, G. Jellinek, J. M. Konieczny, K. C. Kwan, and R. O. Toberman, *ibid.*, **57,** 485(1968).

ACKNOWLEDGMENTS AND ADDRESSES

Received February 17, 1969, from the *College of Pharmacy and Pharmacy Service, University Hospital, The University of Michigan, Ann Arbor,* MI *48104*

Accepted for publication April 2, 1969.